Nguyen, T. and Fellenius, B.H., 2024. Bidirectional static loading tests on barrette piles. A case history from Ho Chi Minh City, Vietnam. Canadian Geotechnical Journal, 59(2) 1-13..

Canadian Geotechnical Journal

Article

Bidirectional static loading tests on barrette piles. A case history from Ho Chi Minh City, Vietnam

Tan Nguyen[a] **and Bengt H. Fellenius**[b]

[a]Faculty of Civil Engineering, Ton Duc Thang University, Ho Chi Minh City, Vietnam; [b]Sidney, BC V8L 2B9, Canada

Corresponding author: **Tan Nguyen** (email: nguyentan@tdtu.edu.vn)

Abstract

Bidirectional static loading tests were conducted on two strain-gage instrumented barrettes installed to 72 m depth in Ho Chi Minh City, Vietnam. The barrettes were to support a 16-storey building with 5 basements. The soil profile comprised layers of medium coarse to fine sand, medium clay, firm to stiff clayey soil, and dense sandy silt. The region is experiencing an ongoing land subsidence affecting the upper about 40 m of soil and, on average in the city, the ground surface is currently settling 16 mm/year. The test records were processed by means of effective stress analysis to provide the axial pile force distribution, load transfer functions, and equivalent head-down load–movement curve. The analysis was then used to obtain the equivalent pile-head load–movement response adjusted to the planned 22 m deep basement excavation. Load transfer functions were back-calculated from the test records and indicate that the construction will show somewhat large load-transfer movement. However, because the equilibrium plane will be below the subsiding layers, below 40 m depth, downdrag is not expected to affect the building. The load response of the barrettes is compared to the results of a bidirectional (BD) loading test on a 1.8 m diameter bored pile at an adjacent project.

Key words: stiffness evaluation, effective stress analysis, equivalent head-down test, load transfer function, impact of different pile geometry

Introduction

Ho Chi Minh City has lately seen an increase in the number of high-rise buildings and long-span bridges, requiring large-diameter bored piles or barrette piles. Due to the complex soil profile and length of piles, the design requires reference to full-scale static loading tests on instrumented piles. This paper reports the results and back-analysis of tests on two barrettes carried out in November 2020. To verify that the test response of the rectangular piles does not differ from that on a circular pile, the results are compared to those of a static loading test on a 1.8 m bored pile carried out in March 2017.

The tests employed the bidirectional method (Elisio 1986; Osterberg 1989; ASTM D8169 2018) due to the costs of an external reaction system for the large maximum test loads. A bidirectional loading test applies loads by means of a bidirectional cell assembly, ideally placed at a depth where the applied load will fully engage the pile resistance both above and below the BD assembly. For other than piles shorter than about 12 m, test piles are usually instrumented for the purpose of determining the force distribution imposed by the applied test loads by locating pairs of strain gages at various depths.

Back-analysis of records from a conventional head-down test on an instrumented pile is affected by the uncertainty of the Young's modulus (E), and of the cross-section (A) of the test pile, which makes the determination imprecise of the pile EA-parameter needed for obtaining the axial force distribution. Moreover, the potential presence of residual force and its distribution at the start of the test makes the actual force values uncertain. This causes the back-calculated force distribution to be inexact in particular in regard to the shaft resistance along the lower depths and the toe resistance. In contrast, the BD-force is independent of both the uncertainty of pile modulus and cross-section and the potential presence of residual force.

The shaft and toe resistances of a pile are proportional to the effective stress distribution and movement relative to the soil. Therefore, an effective-stress back-analysis is necessary for evaluating the response of the result of static loading tests (Fellenius et al. 1999). Moreover, the results of an effective-stress back-analysis can be used to evaluate the effects due to a changed site condition, such as an excavation for basement placement, changes to the groundwater table, etc., which is not possible to do from a stress-independent analysis. If the calculation is carried out in terms of ultimate resistance values of shaft shear and toe stress, the results become additionally distorted as the influence of relative movement is then disregarded.

The objectives of this study are: (i) to present a case study on the static loading tests on two barrettes: TB1 and TB2 (intended to test to a maximum of 65 MN, but terminated at 55 and 58 MN because the movements at these maximum loads

exceeded the BD-cells opening limit), (ii) to compare the response of the barrettes to that of a circular pile, (iii) to address the load–displacement response of the barrettes under various scenarios, such as regional subsidence, and (iv) to evaluate the effect on the foundation response to the planned excavation for a five-storey basement.

Soil profile

The geotechnical site investigation included drilling four boreholes about 50 m apart to 100 m depth with a standard penetration test at every 2.0 m depth. The area was level, varying about 1 m from an average elevation of about +6 m. The soil profile is summarized in Table 1 and Figs. 1 and 2. The groundwater table was located at about 8 m depth and the pore pressure distribution was assumed hydrostatic. Due to mining of groundwater in the area, it is likely that the pore pressure distribution has a slight downward gradient. Layer 4 is indicated as "sand" in the project borehole descriptions. However, this layer is also reported to have a water content of 25% and a compressibility (C_c-e_0) that converts to a Janbu modulus number of 50, which are values not usually found for saturated clean compact sand.

Minh et al. (2015) and Tay et al. (2022) reported that the land subsidence in Ho Chi Minh City is about 16 mm/year. The subsidence occurs mostly in layers above 40 m depth, which include materials ranging from very loose to loose, fine to medium sand, very soft to soft clay, and medium silty clay (Thoang and Giao 2015). The project does not include raising the ground by adding fill or any other site work that could add to the future general subsidence.

Building and foundations

The building proposed for the site comprises 16 storeys above ground and 5 basement floors. The basement foundation level will be at 22.1 m depth. The outer wall will be supported on a 46 m deep, 1.2–1.5 m thick diaphragm wall. Figure 3 shows the layout of the building and its two elevator towers. The foundation design comprises a total of 32 barrettes, each with a cross-sectional size of 1.5 by 6.0 m and 50 m height, i.e., to 72 m depth. Four additional barrettes support a low-rise area extension. These barrettes also measure 1.5 by 6.0 m in cross-section, but the height is reduced to 33 m; i.e., the toe is at 55 m depth.

The barrette piles were cast using polymer stabilizing slurry with viscosity ranging from 40 to 80 (s) measured by Marsh Funnel Viscometer 1500/976cc, and the PH ranged from 8 to 11. Two test barrettes, TB1 and TB2, were provided to assist the foundation design. The test barrettes were provided with a single-level bidirectional cell assembly at depths of 59 and 58 m in TB1 and TB2, respectively. The drilled shafts were cleaned twice using air-lift reverse-circulation method.

The concrete in the barrettes was grade of B45 concrete with 25 MPa compressive strength and 1.45 MPa tensile strength. The reinforcement steel was CB500-V (tensile strength of 435 MPa). The reinforcement consisted of 88 bars, 36 mm in diameter, distributed uniformly along the barrette perimeter. The reinforcement percentage was 1.1%.

Table 1. Soil profile.

Soil layers	Layer 1	Layer 2	Layer 3	Layer 4	Layer 5a	Layer 5b	Layer 6	Layer 7	Layer 8
Description	Soft CLAY	Soft to stiff CLAY with laterite gravel	Soft CLAY with little fine sand and gravel	Stiff to very stiff, fine to coarse SAND with little gravel	Hard CLAY	Sandy CLAY	Fine to coarse SAND and SILT	Hard sandy CLAY,	Fine to medium SAND and SILT
Thickness (m)	1	2–5	3	30	10–14	2–6	24–28	11–12	10 +
Depth (m)	1	≈6	≈9	≈37	≈50	≈56	≈80	≈90	100+
Color and state	yellow-gray	red-brown yellow-gray	gray-yellow brown-red	brown-red gray-white, brown-red	red-brown and yellow-brown	brown-yellow	yellow-red-brown	blue-gray-yellow-brown	yellow brown
N-SPT (blows/0.3 m)	6	6–27	5–7	8–29	30–47	19–29	30–59	31–72	51–78

Table 1. Soil profile

Soil layers	Layer 1	Layer 2	Layer 3	Layer 4	Layer 5a	Layer 5b	Layer 6	Layer 7	Layer 8
Description	Soft CLAY	Soft to stiff CLAY with laterite gravel	Soft CLAY with little fine sand and gravel	Stiff to very stiff, fine to coarse SAND with little gravel	Hard CLAY	Sandy CLAY	Fine to coarse SAND and SILT	Hard sandy CLAY,	Fine to medium SAND and SILT
Thickness (m)	1	2- 5	3	30	10-14	2-6	24-28	11-12	10 +
Depth (m)	1	≈6	≈9	≈37	≈50	≈56	≈80	≈90	100+
Color	yellow-gray	red-brown yellow-gray	gray-yellow brown-red,	brown-red gray-white, brown-red	red-brown and yellow-brown	brown-yellow	yellow-red-brown	blue-gray-yellow-brown	yellow brown
N-SPT [bl/0.3m]	6	6-27	5-7	8-29	30-47	19-29	30-59	31-72	51-78

[Readable copy as per manuscript]

Fig. 1. Soil profile. (A) Soil type and (B) BH2 N-indices.

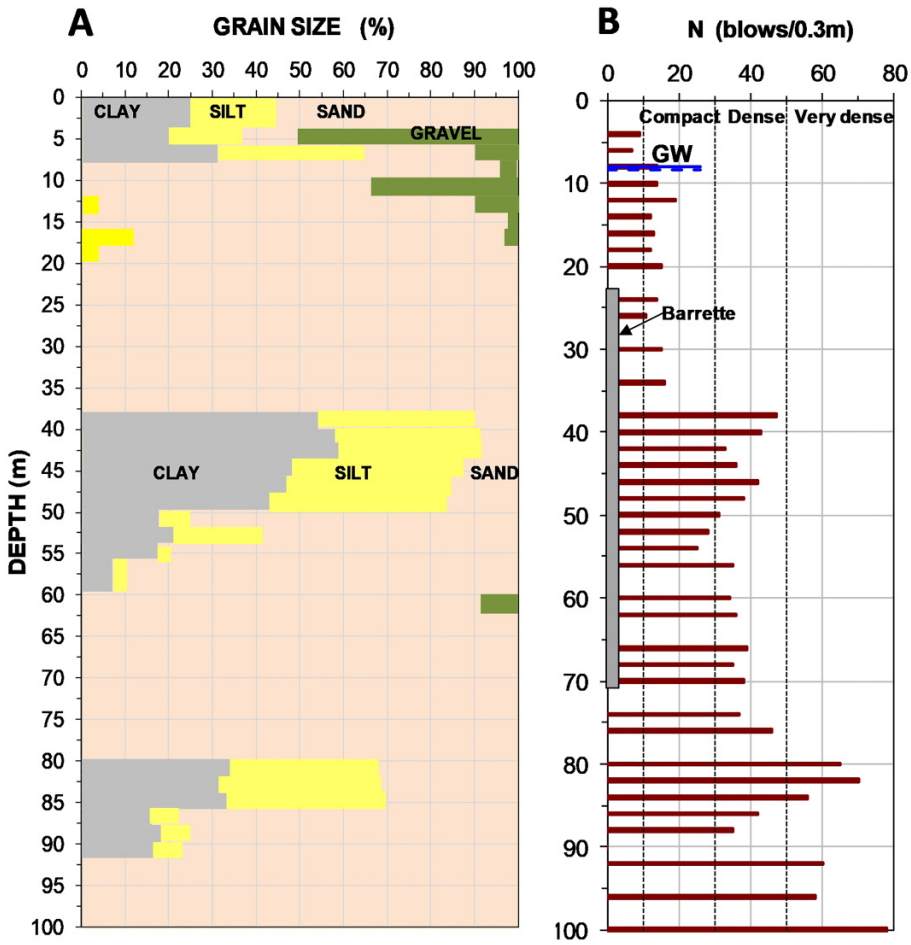

The Vietnam standard 10304-2014 determined the bearing capacity of the barrettes to 130 MN based on the compressive capacity of reinforced concrete. The capacity calculated according to Vietnam standard 10304-2014 from the soil type and SPT N-indices was stated to result in the same capacity. In accordance with the standard, the allowable load was obtained by applying a factor of safety of 2.0. This gave an allowable load (unfactored total load) of 65 MN, subject to confirmation in a static loading test—a bidirectional test. The sustained load assigned to the four shorter barrettes supporting the low-rise area was 36 MN.

According to Vietnam standard 10304-2014, the maximum permitted settlement of the foundations is 100 mm, all conditions considered and, in addition, the maximum unfactored total load must not exceed the test load (head-down test) that resulted in a 40 mm pile head movement. Conventionally, for a bidirectional test, the latter requirement applies to the equivalent head-down test calculated from the results of the bidirectional test (the requirement is addressed below).

The two test barrettes, TB1 and TB2, were constructed from 22 m (the depth of the basement foundation) to 78 m depth in locations indicated in Fig. 3. TB2 will be part of the actual foundation (the space created by the bidirectional test will be grouted on completion of the test). TB1 was not a part.

The vertical movement of the barrette head was measured by LVDTs installed at the pile head and the compression and toe movement were measured using telltales. Vibrating wire-strain gages Geokon Model 4150 and 4120 were placed at eight levels, six at each level. Figure 4 shows the soil profiles and the depths of the strain-gage levels in respect to the borehole profiles.

Ideally, a BD assembly should be placed so that the downward toe movement is at least about 30 mm and the upward pile head movement is at least 5 mm to ensure that the pile resistance is fully engaged. As long as the BD is designed for sufficient movement (travel) and has a margin of force, when allowing a test to continue until both ideal movements have been produced, the BD placement has quite a bit of leeway. Experience of previous tests in the general area in reference to the borehole information led the design to position the BD assemblies for barrettes TB1 and TB2 at 59 m and at 58 m depths, respectively.

Test schedule

The bidirectional tests were carried out in November 2020, 21 days following the completion of pile construction (according to Vietnam standard 9393-2012, a loading test is not permitted to be conducted earlier than 21 days after completed construction). The test method followed Vietnamese

Fig. 2. Distributions of (A) density, (B) water content, and (C) liquid limit and UU.

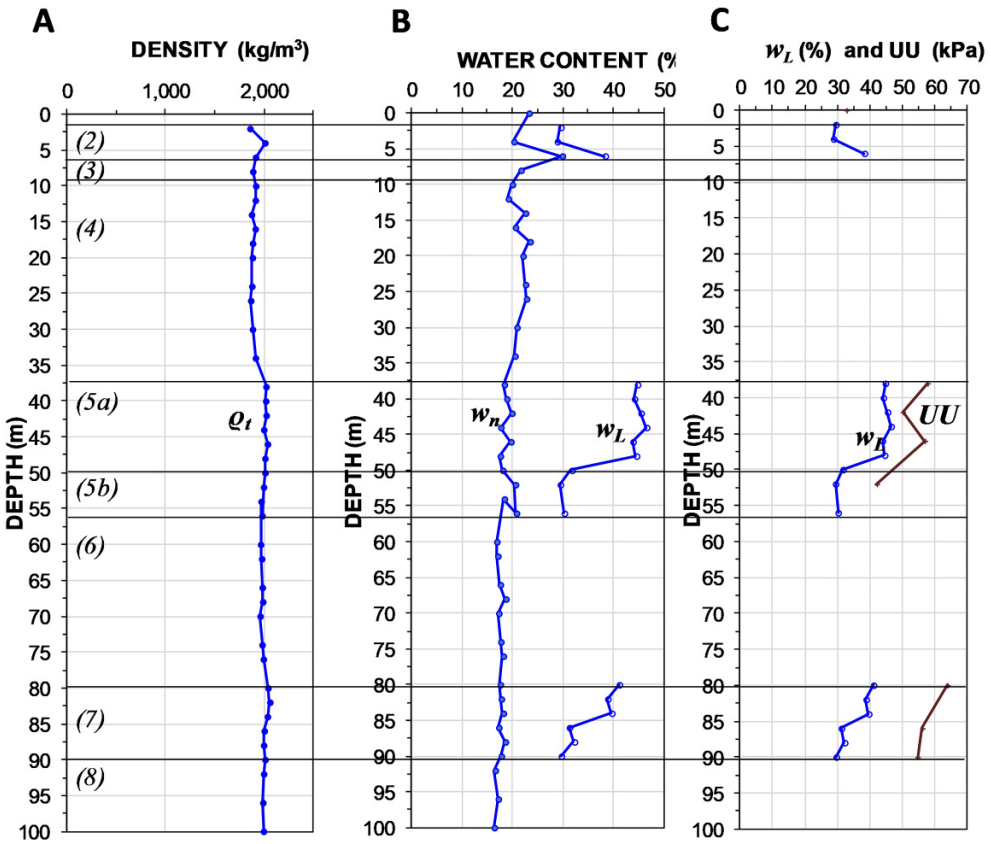

Fig. 3. Site plan and locations of test barrettes TB1 and TB2.

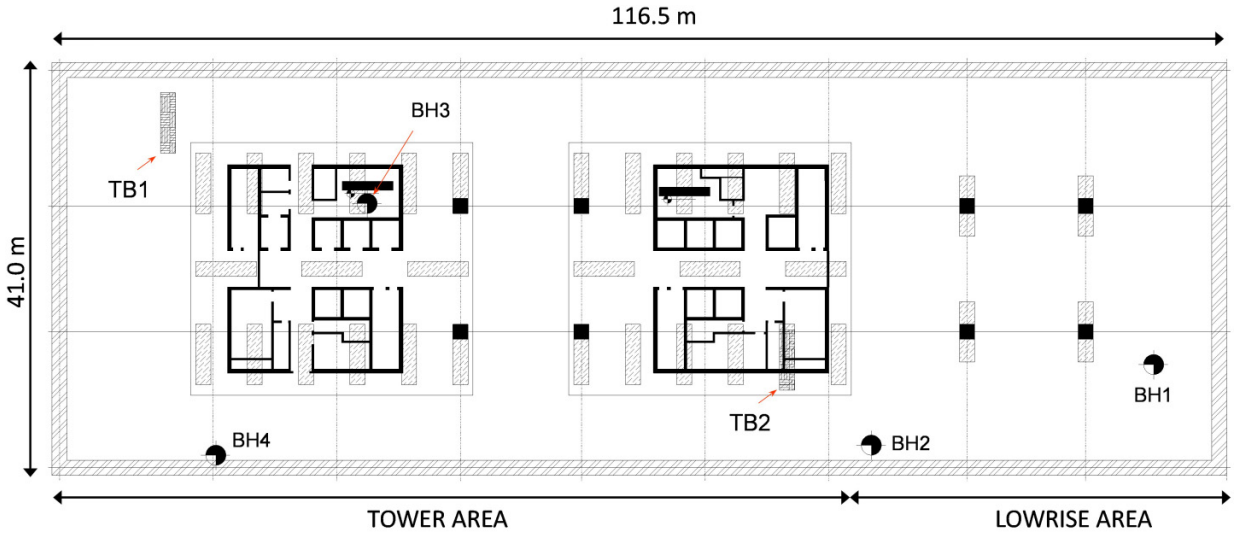

standard 9393-2012, which is similar to ASTM D1143-81, requiring the use of a "maintained-load" method comprising a series of equal load increments and holding each load level steady for certain length of time.

As is frequently the practice in Vietnam, the test schedule included unloading and reloading events and also applying an initial load, 5% of the intended total load to support, held for 10 min, this, ostensibly, to check the operation of test equipment. Such actions build in changes to the strain measurements and adversely affect the interpretation and back-analysis of the test records. Yet, they provide nothing useful for the assessment of the pile response to the applied load (Fellenius and Nguyen 2019; Fellenius 2021, 2024).

Fig. 4. Soil layers with respect to boreholes BH2 (closest to TB2) and BH3 (closest to TB1), pile embedment, and strain gage instrumentation.

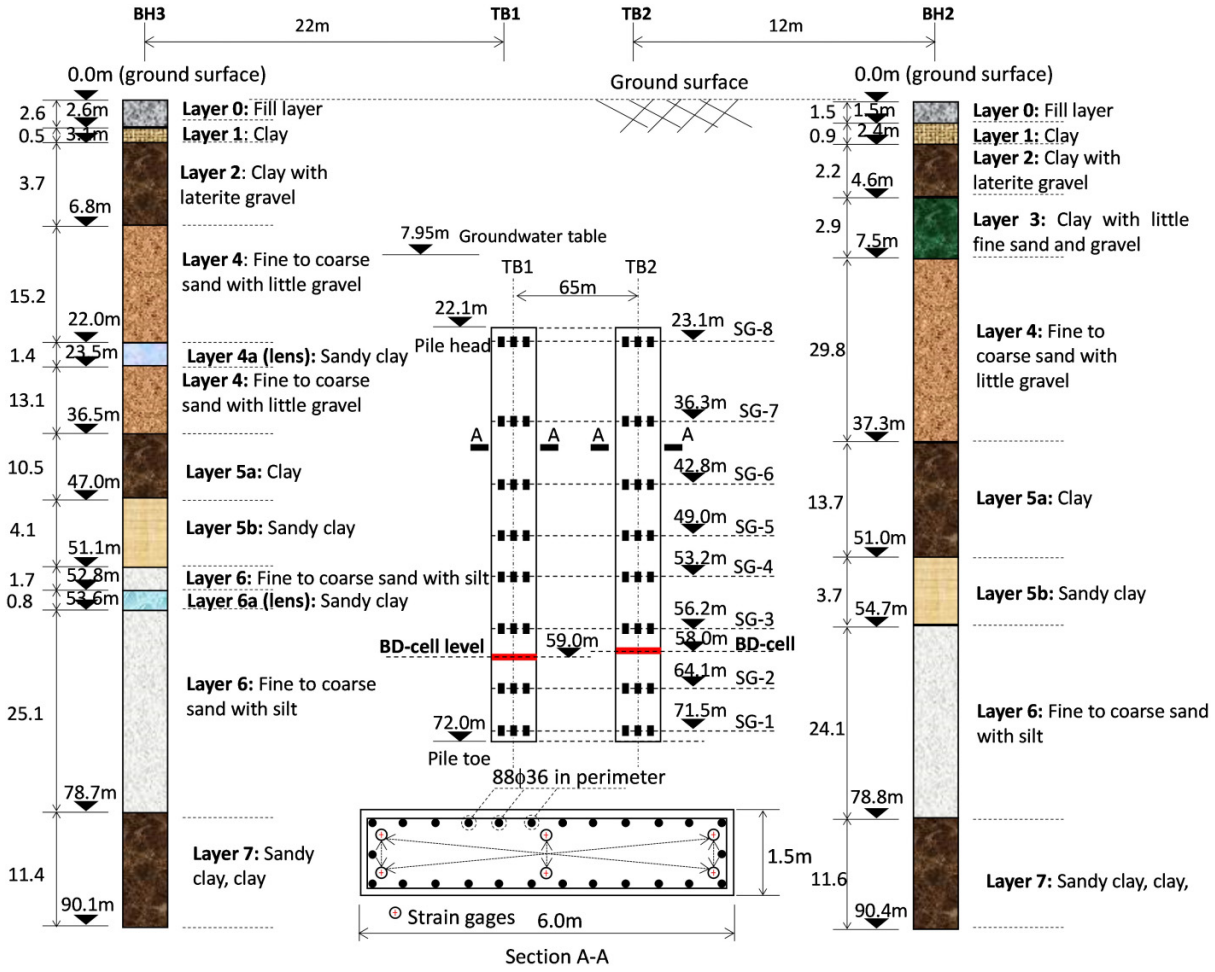

The test schedule and movement-time response of the test barrettes are shown in Fig. 5. Both tests were carried out in two stages: a first stage comprising five equal increments of about 8 MN to a maximum BD load of about 38 MN (half the 65 MN unfactored foundation load to support) followed by unloading and, then, a second stage, omitting the first 8 MN increment and, starting at 8 MN, applying six increments of about 8 MN to a maximum load of about 55 and 59 MN, when the tests were terminated because the movements exceeded the BD-cell opening limit. The load-holding duration was 2 h for Stage 1 and 0.5 h for Stage 2, but for the last two load levels, when the loads were held longer (the maximum load was held for about 20 h, although it kept dropping for TB1, but without increase of movement, indicating pump issues). The unloading–reloading events, uneven loads, and load-holding durations are regrettable. Not applying equal increments of load, maintaining equal load-holding duration, and including unloading–reloading events impair the quality of the test records and make the back-analysis less precise (Fellenius 2017; Fellenius and Nguyen 2019; Fellenius and Ruban 2020).

Test results

Figure 6 shows the measured load–movement response of the tests. The downward curves are plotted per the full BD load and the upward curves are plotted after subtracting the buoyant weight of the barrette. The curves show the movement during each load-holding event. The holding time was at first 30 min and, then, changed to 2 h. Movement increased for TB1 during the holding time, but not for TB2, but no explanation was provided for this difference in the field records. The results are very similar for the two test barrettes. The slightly smaller upward movement of TB1 and slightly larger downward movement as compared to TB2 are likely due to the 1.0 m difference in the depths to the BD-cell assembly. The recorded compression of the barrettes for the load was small, at maximum load about 3 mm both downward and upward. The labels “L2-4” and “2L-5” refer to the second test stage and fourth and fifth load levels, respectively. The load–movement of TB1 after L2-6 was erratic and is not plotted.

The strains imposed during the test were measured and can be converted to force by multiplication with the barrette EA-parameter (E is the material modulus and A is the pile cross-

Fig. 5. The load increments and BD-cell movements during the tests.

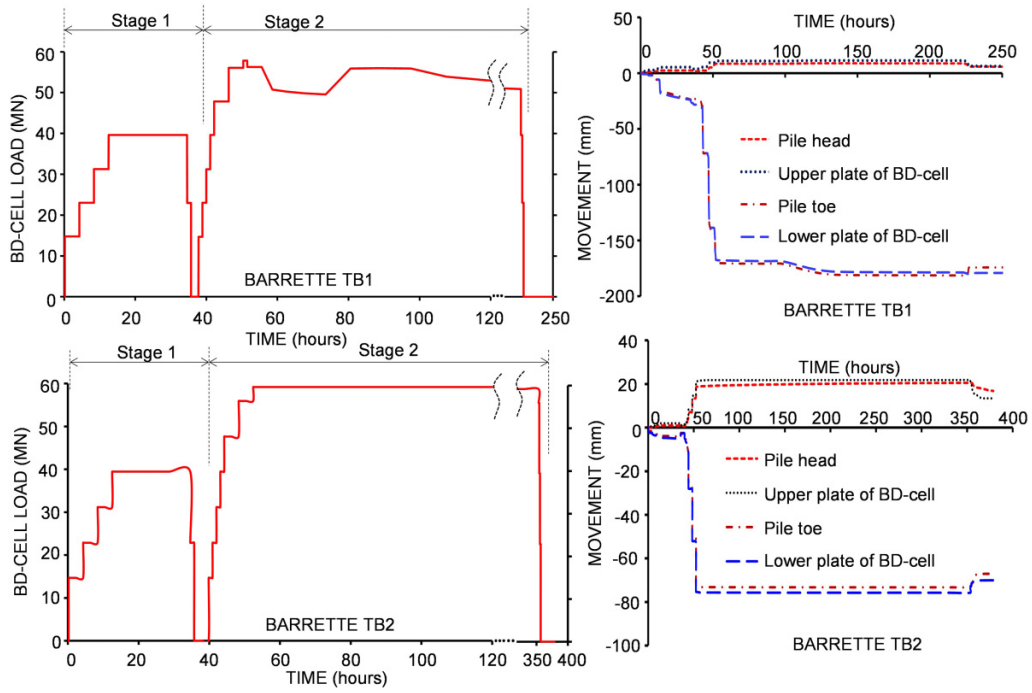

Fig. 6. TB1 and TB2 load–movements (N.B. movement scales differ for upward and downward graphs).

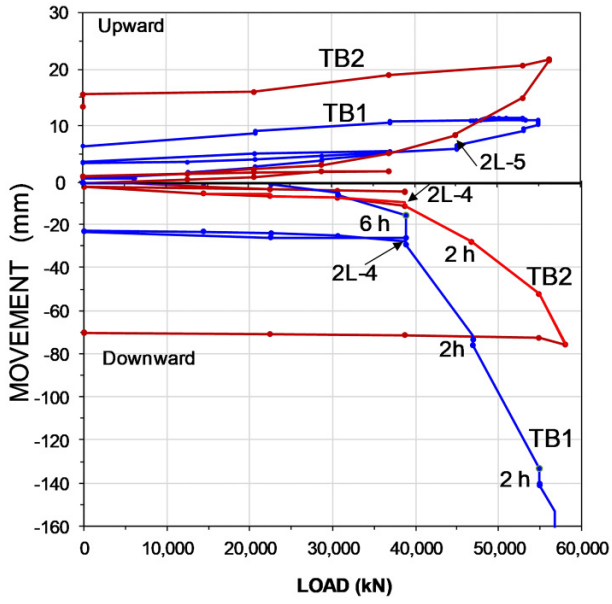

sectional area). It is likely that the actual barrette breadth and width deviated from the nominal values and A is not quite the nominal 9.0 m^2 value. As the barrettes were reinforced, the modulus is a combination of the E-modulus of the steel and concrete. Moreover, while the E-modulus of the steel is well known, the modulus of the concrete can vary within a wide range and, furthermore, it may also vary with the stress level. More important, the modulus can differ significantly from a value determined from the concrete properties, notably, the strength. According to ACI318-19 (22), the E-modulus (MPa) of ordinary weight concrete is $4700\sqrt{f'_c}$ (thus, a modulus of 23.5 GPa and an EA-parameter of 210 GN). Other standards indicate slightly different relations for determining E-modulus from concrete strength.

For a head-down test, the stiffness can be determined from the actual load–strain measurements obtained for a strain level close to the pile head, where the load–strain response is unaffected by shaft resistance. In contrast, a gage level close to the BD assembly is affected by shaft resistance. However, when the relative movement between the shaft and the soil has been large enough, usually just a few millimetres, for the load–strain curve to become approximately linear, and provided that the shaft resistance exhibits a plastic response, the slope is then the axial stiffness. Also for other strain-gage levels, once the shaft response has been mobilized to a plastic state, the load–strain slope may provide the EA-parameter as an expression of the pile stiffness. However, when the shaft shear response is nonplastic, i.e., when strain-hardening or strain-softening, the slope of the stress–strain curve becomes steeper or less steep than true, respectively. The back-analysis of pile axial stiffness from the test records is then difficult (Fellenius 2024).

Whether or not the shaft shear response is plastic can be estimated from a plot of the "tangent EA-parameter", which is the change of load divided by the change of strain plotted versus the strain for the load increments. For an ideally plastic shaft resistance, the tangent EA-parameter after full mobilization of the shaft resistance will be an essentially horizontal line, sometimes with a slight slope due to a reduction of concrete modulus with increasing strain (Fellenius 1989, 2024). The tangent EA-parameter, being a differentiation method, requires accurate records of load and strain. A

Fig. 7. TB1 and TB2 load–strain and tangent EA-parameter.

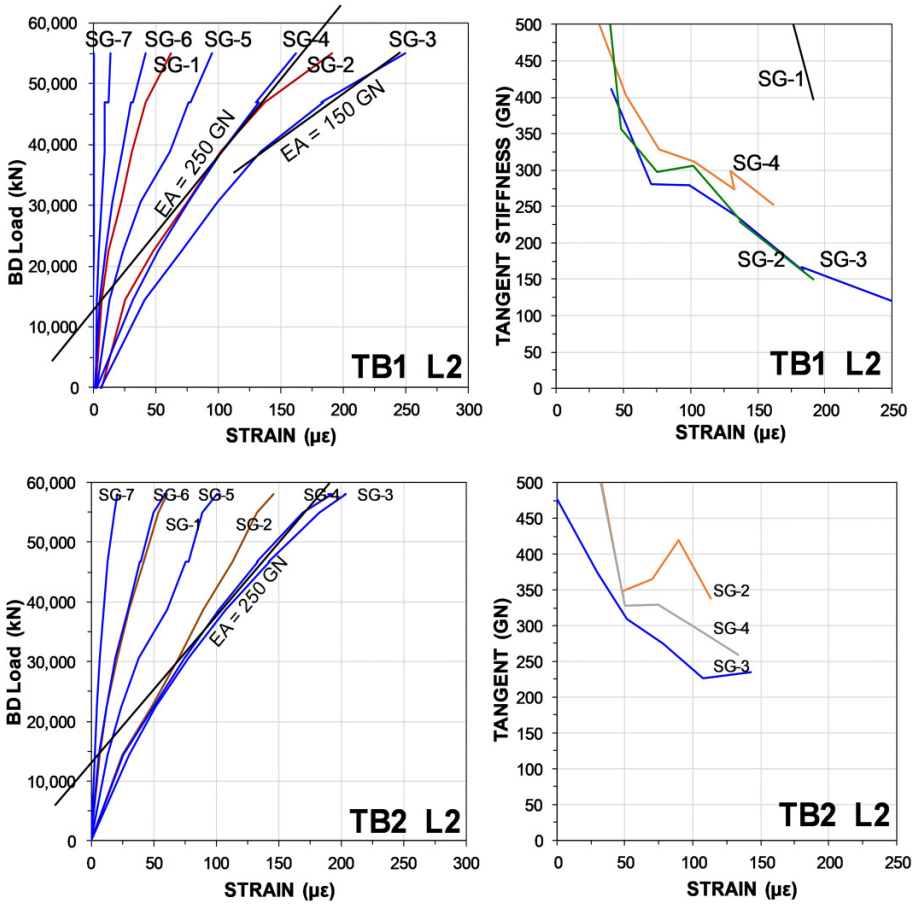

Fig. 8. TB1 and TB2 distributions of beta-coefficient.

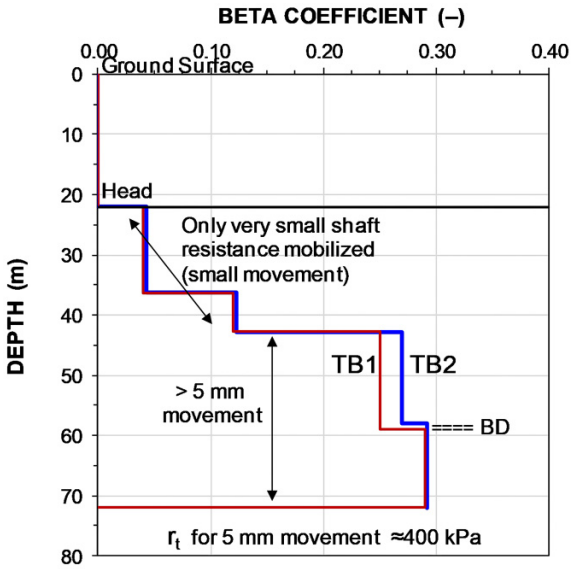

tangent modulus increasing with increasing strain is an indication of strain-hardening and vice versa for decreasing slope. This is more pronounced the longer the distance is between the generating force (BD-cell assembly or jack) and the strain-gage level.

The fact is, however, that many soils do not exhibit plastic response and, therefore, what actual EA-parameter to use for the conversion is often uncertain (Fellenius 1989, 2024). Moreover, the EA-parameter is also affected by the testing schedule. Tests that include unloading and reloading events or load-holding durations that are not constant for levels of applied load will have strain records that cannot be converted to force as reliably as for tests carried out not using an inconsistent schedule (Fellenius 2017, 2018).

Figure 7 shows the load–strain and tangent EA-parameter graphs plotted from the records. The load–strain slopes are nearly linear toward the end of the test, but the slopes are far from parallel. The line marked 150 GN would, theoretically, imply an E-modulus of 16 MPa for the barrette material, which is not likely true for the concrete used in the barrettes. The slope of the load–strain lines marked EA = 250 GN is reasonable. An EA of 250 GN would represent an E-modulus of 28 GPa of the barrette, including the effect of the reinforcement. However, the fact that the tangent EA-parameter graphs show no trend toward a steady stiffness, which would be indicated by a horizontal or only slightly sloping line, indicates that either the strain records are affected by the unloading–reloading events and/or the shaft resistance response did not show a plastic state in one or more

Fig. 9. TB1 and TB2 force distributions in Stage 2 for EA = 250 GN.

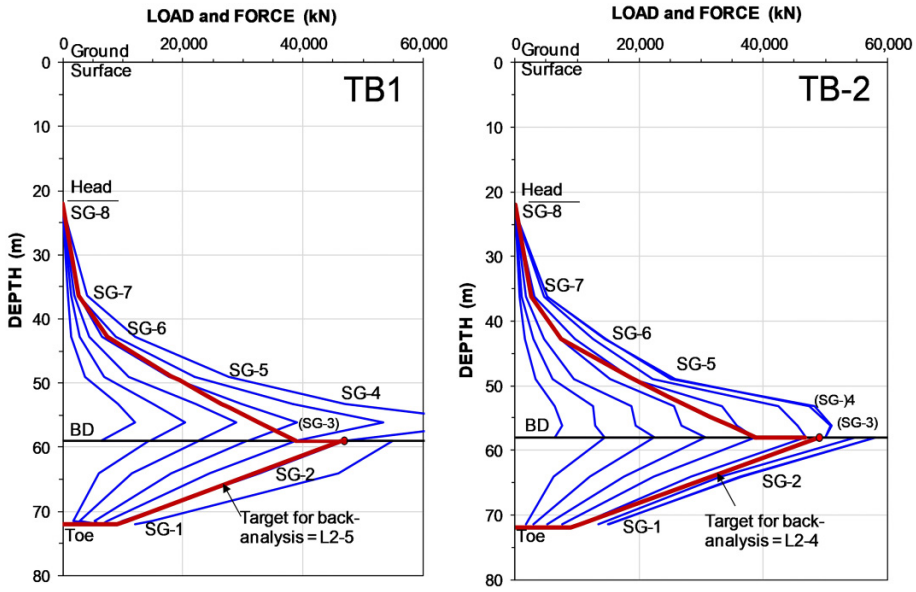

Fig. 10. Measured and simulated load–movement curves (N.B. movement scales differ for upward and downward graphs).

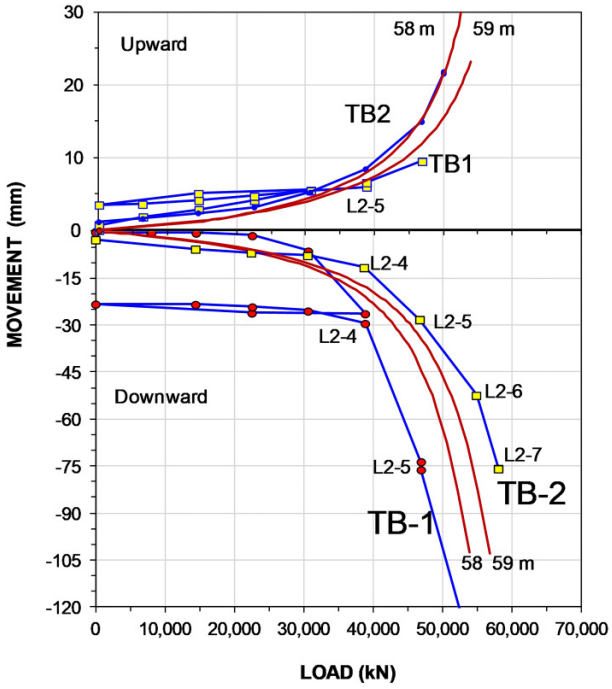

of the soil layers between the BD-cell assembly and the strain-gage level. For details about methods of assessing pile axial stiffness, see Lam and Jefferis (2011) and Fellenius (2012, 2024).

The authors prefer to apply an innovative alternative option for determining the axial stiffness. The method comprises designating one or two of the applied loads as target load and calculating the force distribution above and below the BD-cell assembly for the target loads from the strain-gage records, applying an EA-parameter that provided the best match to the force distribution between the pile head and the BD load, the latter being a true axial force and the distribution below the BD assembly. The target BD loads were chosen to be for about 5 mm movement, Stage 2, Load 5 (L2-5) upward and 2L-4 and 2L-5 downward. The fitting aimed to produce a realistic distribution between the BD load, which is true load, and the pile head, where the force is zero, of course, also a true load. The process recognizes the soil layering by coupling the calculations by assigning a specific beta-coefficient to each soil layer and performing the fitting process in an effective stress calculation incorporating the density of each soil layer and the depth to the groundwater table assuming hydrostatic pore pressure distribution. For each soil layer, the assigned beta-coefficient was adjusted to fit the applied BD load and to produce a realistic force distribution between the BD load and the zero load at the pile head. The calculation method to achieve the distributions is a straight-forward, though laborious, effective-stress analysis performed in a spreadsheet.

The procedure of matching the target BD load resulted in distributions of beta-coefficients and unit toe resistance, r_t, shown in Fig. 8 for 5 mm pile element movement. Figure 9 shows the axial force distributions (heavy lines) calculated from the fitted parameters.

The distributions were then related to the strain-gage records for the target load and an average EA-parameter that best fitted the distribution was determined. For TB1, the EA-parameters were 290 GN for the length above and 240 GN below the BD assembly, correlating to E-moduli of 32 and 27 GPa, respectively, for the nominal barrette cross-section. For TB2, the values were 225 and 240 GN for the lengths above and below the BD assembly, respectively, correlating to E-moduli of 25 and 27 GPa, respectively, for the nominal barrette cross-section. The so calibrated EA-parameters were then used to calculate the axial forces from the strain-gage

Fig. 11. The t-z and q-z curves used for the load–movement simulations.

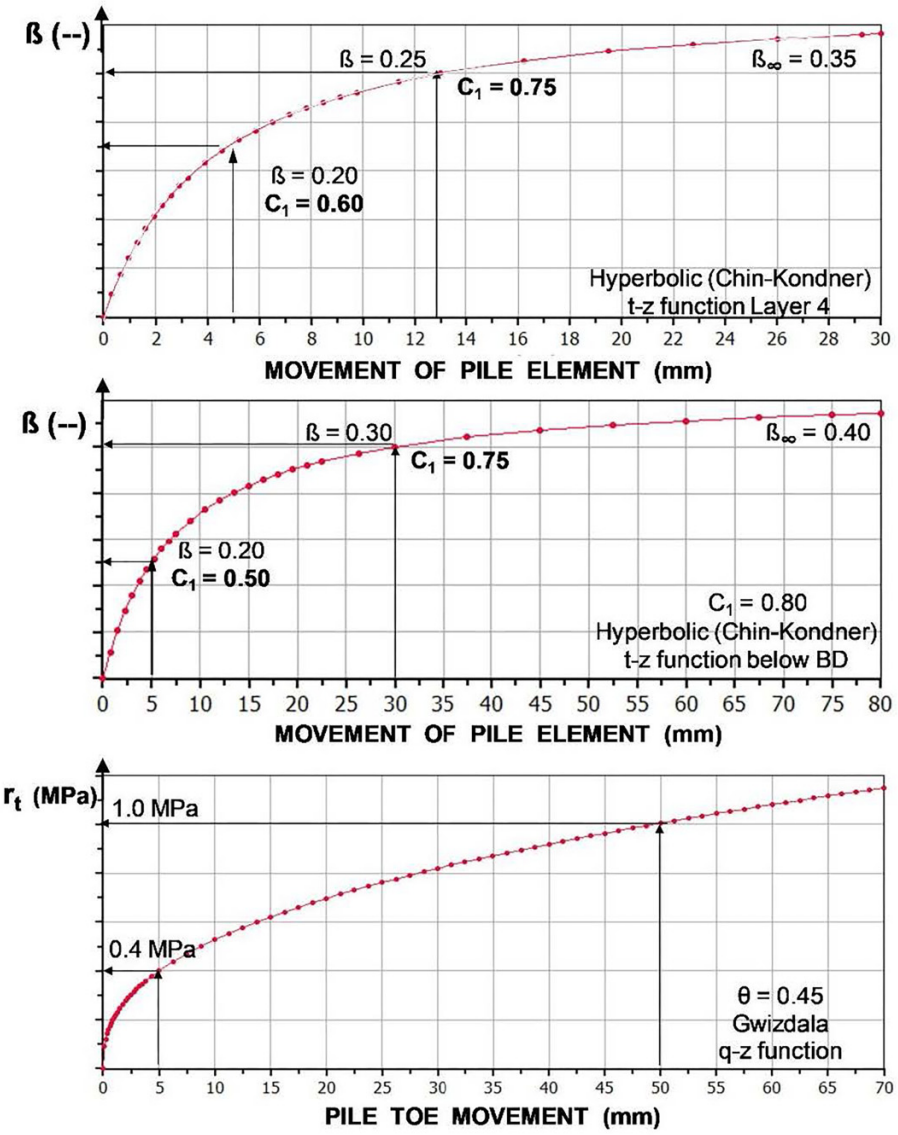

records produced by the other applied loads, as shown by the fans of thin curves.

Figure 10 shows the measured load–movements (curves with symbols) together with the simulated curves (curves with no symbols) applying t-z and q-z functions obtained by the described fitting approach. Two simulated curves are shown because the simulation was made for two different depths to the BD assembly, 58 and 59 m, respectively. Because of the uncertainty of measured values caused by the variable testing schedule, the same beta-coefficients, average of those fitted to the force distribution, and the same t-z and q-z functions were applied to both tests. It would have been entirely possible to produce simulated curves that fitted each test perfectly. However, the fine fit of that analysis would have been mainly cosmetic. The results of the two tests are essentially identical. The difference between the results is mostly due to the loose testing schedule and to the 1 m difference in depth to the BD assembly. The fit between the calculated load–movement curves to the measured curves was made using the UniPile software (Goudreault and Fellenius 2014).

Figure 11 shows the t-z and q-z functions developed for the fit of simulated load–movement curves to the mean of the measured curves. The curves have been supplemented with identification of beta-coefficients and unit toe resistance versus and pile-element movement. They also include values for $ß$ and r_t for movements larger than 5 mm. The simulation fit enabled estimating the beta-coefficients for movements smaller as well as larger than those measured for the target load. The results show that the measured soil response was strain-hardening as opposed to the usually assumed plastic response.

The function curves shown in the figure could also have been expressed in terms of unit shaft resistance within each of the soil layers, which, then, would have varied from the upper to the lower boundaries of the layers, or as an average value for each layer, which, if correlated to a beta-coefficient,

Fig. 12. Equivalent head-down load–movement curves.

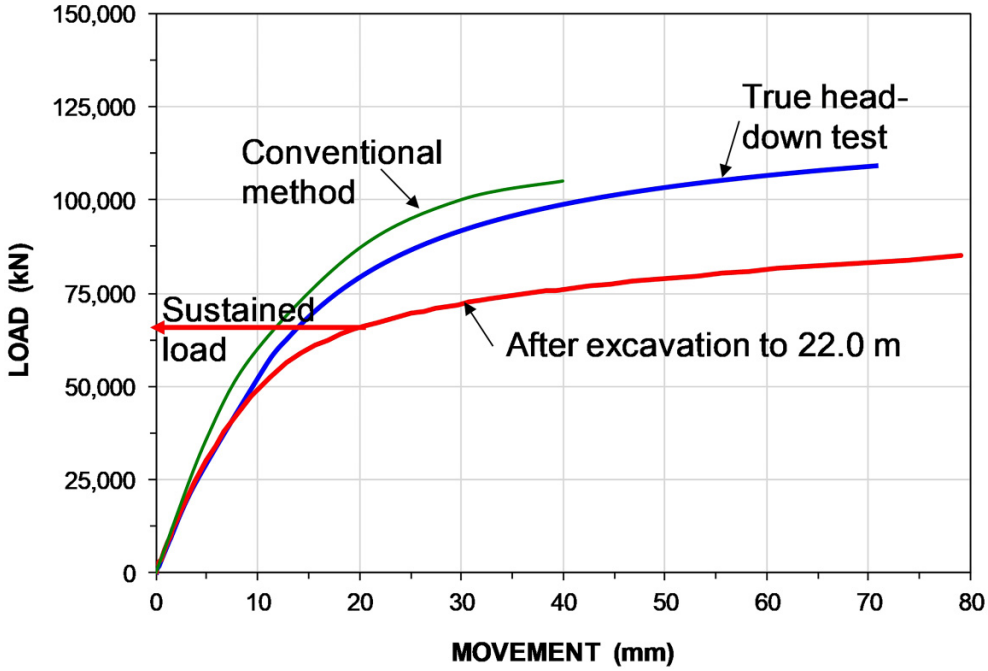

would have shown them to vary from the upper to the lower boundaries of the layer. The important realization is that neither the unit shaft resistances nor the beta-coefficients represent an ultimate resistance. The values are governed by the relative movement between the pile and the soil.

It is common to produce an "equivalent head-down test" from the results of a bidirectional test. The conventional procedure consists of adding the applied upward and downward loads for equal values of measured movements. The so-determined load–movement curve is then adjusted by adding the calculated shortening of the pile to account for the fact that the head-down test involves transmitting the load acting below the BD assembly from the pile head through the length of the pile above the BD assembly. The adjusted load–movement curve is conventionally considered to be the "equivalent head-down curve". However, in the BD test, the elements nearest above the BD level are engaged first, while in a head-down test, they are engaged later in the test. Therefore, where the soil response for the pile elements nearest the ground is softer than for those nearest the BD, the calculated equivalent head-down curve will show a stiffer than true response. The difference can be significant and result in an overestimation of the pile capacity ("failure load"), when applied to the equivalent head-down curve.

Figure 12 shows the equivalent head-down load–movement curves determined by applying the t-z and q-z functions obtained from fitting theoretical calculation to the measured response of the pile. The initial rise shown by the conventional method implies a stiffer response than the slightly softer response shown by the "true curve" that considers the fact that the head-down curve engages the upper layers first.

Most important is that the future actual conditions at the site for the foundation barrettes will include a 22 m deep excavation, which will reduce the effective stress and, therefore, reduce the stiffness of the barrette response. This is frequently not recognized by foundation designers, in only considering the future excavation either by not having the pile constructed above the depth of the excavation (as here) or by subtracting the resistance between the ground surface and the excavation depth. The "After excavation" curve in Fig. 12 shows the results when the unloading effect of the excavation is considered. It would seem that the load-transfer movement of the barrette foundations for the intended sustained load (65 MN) might be rather large. However, the pile head movement is still only half of that permitted by the Vietnam standard, as mentioned. We recommended that the settlement of the foundations be monitored during the construction. The recommendation was not considered persuasive.

The post-excavation load–movement curve is an extrapolation of the test analysis and, therefore, less certain than the actual test. Moreover, the excavation will have turned the soil from being normally consolidated into a preconsolidated state, which might increase the foundation stiffness to the applied load.

The back-analysis of the tests shows that the toe of the barrettes provided a good response. In the long term, therefore, the equilibrium plane (force and settlement equilibriums) will likely be below about 50 m depth, i.e., below the layers generating the general subsidence at the site and the barrettes will move down to mobilize the toe bearing associated with increased toe movement. Thus, the foundations will settle in addition to the load-transfer movement.

Fig. 13. N-index diagram and soil profile of TP1 at the adjacent building.

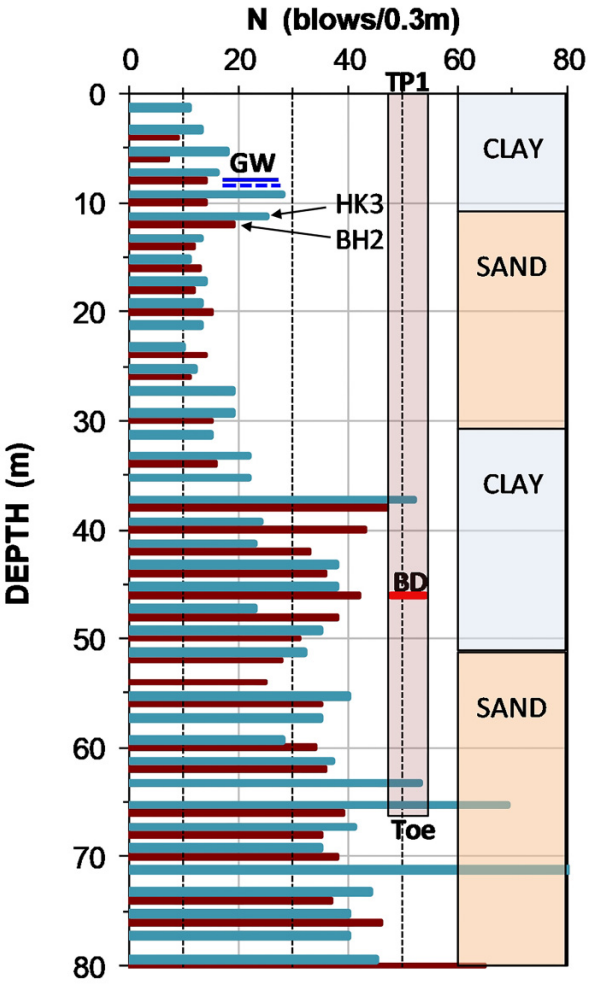

Comparison to the response of a bored pile

The site adjacent to the subject site included a static loading bidirectional test on an 1800 mm diameter, 66 m long bored pile (TP1), constructed under polymer slurry at an about 100 m distance from the current site, which gave an opportunity to compare the response of the barrettes to that of a bored pile. The concrete cube strength was reported as 60 MPa, considerably more than the concrete strength (25 MPa) reported for the barrettes. According to the ACI relation, the concrete E-modulus would have been 36 MPa and the parameter, EA, 90 GN. The soil profile at the adjacent site is very similar to that at the subject site. Figure 13 shows the soil profile and a diagram of N-indices from a borehole (HK3) at the adjacent site supplemented with the N-indices from BH2 at the current site. The "BD" indicates the location of the bidirectional cell assembly.

The loading test (January 2017) followed the same schedule as used for the barrette tests. Figure 14 shows the schedule (load vs. time) and measured upward and downward movements versus time for the BD plates. The label "2L-8" indicates the applied load chosen as target for the back-analysis, i.e., Stage 2, Load 8.

The strain-gage records were similarly affected by the unsuitable loading schedule and three gage levels were very off. The back-analysis of the pile axial stiffness was therefore made according to the same innovative approach as used for the barrettes. The stiffness analysis produced an EA-parameter of 44 GN for the strain-gage conversion to axial force, but for the mentioned three gage records (c.f., Fig. 15A). Applying a stiffness calculated according to the ACI relation would have considerably overestimated the axial forces. The strain values converted to force showed a good agreement with the distribution for the target load. However, an EA of 44 GN represents an E-modulus of a mere 17 GPa for the nominal pile cross-section (2.55 m^2), about half of the expected value. It is outside the scope of this paper to determine why this overly low value would appear.

Figure 15B shows a comparison between the measured load–movement curves and the curves produced by fitting t-z and q-z functions to the measured curves. The fits were obtained using the same t-z functions as shown in Fig. 10. The toe response, however, required using a Gwizdala function coefficient of 0.70 as opposed to 0.45.

Comparing the analysis results of the barrettes and the circular pile shows that there was no fundamental difference in response between the rectangular and circular shapes. The effective stress parameters back-analyzed from the test records were very similar and the shaft resistance was strain-hardening for both the barrettes and the bored pile.

Summary and conclusions

1. The back-analysis of the load and strain records showed that the unloading–reloading event included in the test schedule and the strain-hardening soil response prevented obtaining a good value of the pile EA-parameter from the slope of the load–strain versus strain records or from the tangent modulus method.
2. The alternative of determining the pile stiffness using the ACI relation to the concrete strength did not result in a realistic distribution of axial pile force.
3. The pile stiffness was instead determined from a novel method that (A) relies on the fact that the bidirectional cell load is true load unaffected by variation in the testing schedule, residual force, recording issues, etc., which enabled establishing a realistic force distribution between the BD assembly level and the pile head with reference to the soil profile, and (B) fitting an axial stiffness common for the full length of the pile to the force distribution for a chosen applied load, a target load, excluding values with obvious error.
4. A target load was chosen as the applied load that resulted in an average of about 5 mm movement between the pile elements and the soil. The force distribution for the target load was then correlated to distribution of shaft resistance in terms of beta-coefficients (ß) and unit shaft resistances.
5. The shaft resistances for 5 mm movement in the soil layers were then used as pivot point for relation of shaft resistance to relative movement of the pile elements expressed in t-z and q-z functions, which, when fitted to

Fig. 14. Load–time schedule and measured BD movement versus time for TP1 test.

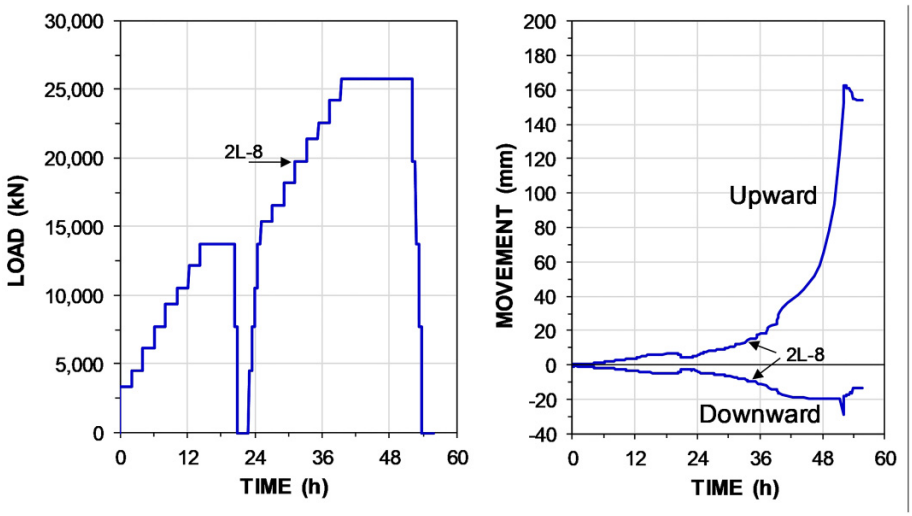

Fig. 15. (A) Force distribution for 2L-8 and (B) movement versus load as measured and as produced by fitting t-z and q-z functions to produce simulated test curves.

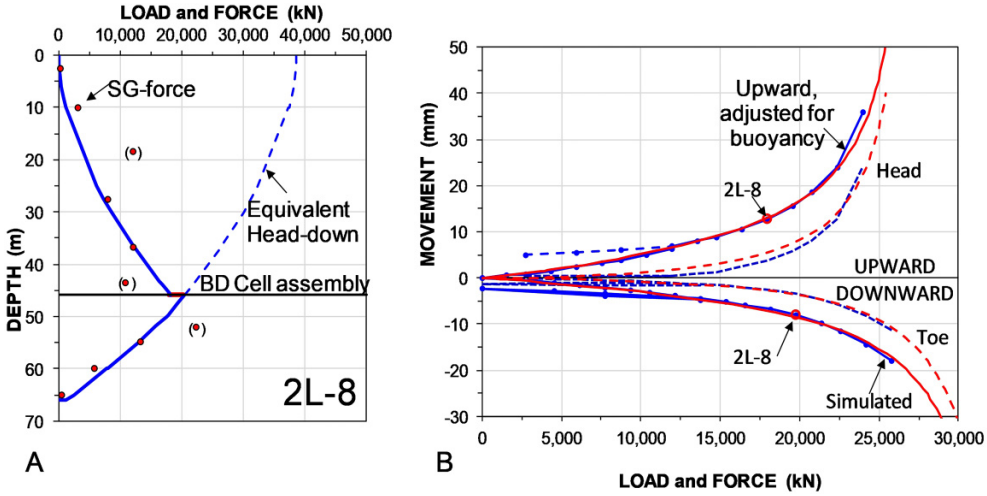

the measured upward and downward load–movement curves, established the function parameters.

6. The good agreement between the measured and simulated test results enabled a simulation of the load–movement curve for the "equivalent head-down test". This was compared to the conventional method for determining the equivalent head-down test and confirmed the conclusion that the conventional method results in an unrealistically stiff curve.
7. The similar analysis of the results of the pile test at the adjacent site showed that the pile shape, i.e., rectangular or circular, had no effect on the soil response in terms of ß-coefficients, unit shaft resistances, and t-z and q-z principles.
8. Performing the analyses applying effective stress parameters (σ'_v and ß) enabled simulating the head-down load–movement after basement excavation, showing reduction of bearing. The conclusion from the so-determined curve is that the fully constructed building might experience excessive movement—settlement.
9. It is concluded that the back-analysis approach and the novel analysis method can be used to estimate the response of other foundations and piles for adjacent foundations.
10. It is concluded that the general subsidence at the site will result in downdrag that will cause the pile toe to move until sufficient toe resistance has developed to move the equilibrium plane to below the subsiding soil layers.

Acknowledgements

This research has received funding from Ton Duc Thang University under the Grant Contract Number FOSTECT.2022.06. This financial support is gratefully acknowledged. The first author extends sincere gratitude to Dr. Minh-Tung Tran (Ton

Duc Thang University) and to his close friend Mr. Huynh Van Vien (REE Corp). Mr. Vien's strong interest in advancing piled foundation understanding in Vietnam made him provide the data for this study. Additionally, the authors express thanks to the anonymous reviewers for their valuable comments.

Article information

History dates

Received: 2 March 2023
Accepted: 4 January 2024
Accepted manuscript online: 10 January 2024
Version of record online: 4 March 2024

Copyright

Data availability

The data that support the findings of this study are available on request from the corresponding author.

Author information

Author ORCIDs

Tan Nguyen https://orcid.org/0000-0003-4909-4258

Author contributions

Conceptualization: TN, BHF
Data curation: TN, BHF
Formal analysis: TN
Funding acquisition: TN
Investigation: TN, BHF
Methodology: TN, BHF
Project administration: TN
Resources: TN
Software: BHF
Supervision: BHF
Validation: BHF
Visualization: TN, BHF
Writing – original draft: TN, BHF
Writing – review & editing: BHF

Competing interests

The authors declare that they have no known competing financial interests or personal relationships that could have appeared to influence the work reported in this paper.

References

ASTM D8169. 2018. Test methods for deep foundations under bi-directional static axial compressive load. Annual book of ASTM standards, Part 19. 13p.

Elisio, P.C.A.F. 1986. Celula expansiva hidrodinamica; uma nova maneira de ecutar provas de carga (hydrodynamic expansion cell: a new way of performing loading tests). *In* Proceedings of VIII Congresso Brasileiro de Mecânica dos Solos e Engenharia de Fundações, VIII COBRAMSEF, Porto Alegre, Brazil, October 12–16, 1986. Vol. 6. pp. 223–241.

Fellenius, B.H. 1989. Tangent modulus of piles determined from strain data. ASCE, Geotechnical Engineering Division, the 1989 Foundation Congress. Vol. 1. *Edited by* F.H. Kulhawy. pp. 500–510.

Fellenius, B.H. 2012. Critical assessment of pile modulus determination methods. Canadian Geotechnical Journal, **49**: 614–621. doi:10.1139/t2012-027.

Fellenius, B.H. 2017. Best practice for performing static loading tests. Examples of test results with relevance to design. *In* 3rd Bolivian International Conference on Deep Foundations, Santa Cruz de la Sierra, Bolivia, April 27–29. Vol. 1. pp. 63–73.

Fellenius, B.H. 2018. Pitfalls and fallacies in foundation design. Innovations in Geotechnical Engineering, ASCE GSP 299 honoring Jean-Louis Briaud. *Edited by* X. Zhang, P. Cosentino and M. Hussein. ASCE GeoInstitute, ADSC, DFI, and PDCA, Int. Found. Congress and Equipment Exposition, Orlando, March7. pp. 299–216.

Fellenius, B.H. 2021. Comments on analysis of a static loading test. IPA Newsletter, Invited Special Contribution, **6**(3): 23–30.

Fellenius, B.H. 2024. Basics of foundation design—a textbook. Electronic Edition, 548p. Available from https://www.fellenius.net/.

Fellenius, B.H., Altaee, A., Kulesza, R., and Hayes, J. 1999. O-cell testing and FE analysis of 28-m-deep barrette in Manila, Philippines. Journal of Geotechnical and Geoenvironmental Engineering, **125**(7): 566–575. doi:10.1061/(asce) 1090-0241 (1999) 125:7 (566).

Fellenius, B.H., and Nguyen, B.N. 2019. Common mistakes in static loading-test procedures and result analyses. Geotechnical Engineering Journal of the SEAGS & AGSSEA, September 2019, **50**(3): 20–31.

Fellenius, B.H., and Ruban, T. 2020. Analysis of strain-gage records from a static loading test on a CFA pile. DFIJ, **14**(1): 39–44. doi:10.37308/DFIJnl.20181008.189.

Goudreault, P., and Fellenius, B. 2014. UniPile Version 5, User and Examples Manual. UniSoft Geotechnical Solutions Ltd.

Lam, C., and Jefferis, S.A. 2011. Critical assessment of pile modulus determination methods. Canadian Geotechnical Journal, **48**: 1433–1448. doi:10.1139/t11-050.

Minh, D., Van Trung, L., and Toan, T. 2015. Mapping ground subsidence phenomena in Ho Chi Minh City through the radar interferometry technique using ALOS PALSAR data. Remote Sensing, **7**(7): 8543. doi:10.3390/rs70708543.

Osterberg, J. 1989. New device for load testing driven piles and bored piles separates friction and end-bearing. Deep Foundations Institute. *In* Proceedings of the International Conference on Piling and Deep Foundations, London, June2–4. Vol. 1. *Edited by* J.B. Burland, J.M. Mitchell and A.A. Balkema. pp. 421–427.

Tay, C., Lindsey, E.O., Chin, S.T., McCaughey, J.W., Bekaert, D., Nguyen, M., et al. 2022. Sea-level rise from land subsidence in major coastal cities. Nature Sustainability, **5**(12): 1049–1057. doi:10.1038/s41893-022-00947-z.

Thoang, T.T., and Giao, P.H. 2015. Subsurface characterization and prediction of land subsidence for HCM City. Engineering Geology, **199**: 107–124. doi:10.1016/j.enggeo.2015.10.009.